

Linköping University Postprint

**Renal Artery Stenosis: Extracting
Quantitative Parameters With a
Mathematical Model Fitted to Magnetic
Resonance Blood Flow Data**

Martin Larsson, Anders Persson, Per Eriksson, Johan Kihlberg, Örjan Smedby

Original publication:

Martin Larsson, Anders Persson, Per Eriksson, Johan Kihlberg, Örjan Smedby, Renal Artery Stenosis: Extracting Quantitative Parameters With a Mathematical Model Fitted to Magnetic Resonance Blood Flow Data, 2008, Journal of Magnetic Resonance Imaging, (27), 1, 140-147.

<http://dx.doi.org/10.1002/jmri.21232>.

Copyright: John Wiley and Sons, Inc,

<http://www3.interscience.wiley.com/journal/10005199/home>

Postprint available free at:

Linköping University E-Press: <http://urn.kb.se/resolve?urn=urn:nbn:se:liu:diva-10712>

Renal Artery Stenosis: Extracting Quantitative Parameters With a Mathematical Model Fitted to Magnetic Resonance Blood Flow Data.

Martin Larsson, Medical student¹, Anders Persson, M.D., Ph.D.¹, Per Eriksson, M.D., Ph.D.², Johan Kihlberg, R.N., Radiographer, M.A.¹, Örjan Smedby, Dr.Med.Sci.^{1,3}

¹ Center of Medical Image Science and Visualization (CMIV), Linköping University, Linköping, Sweden

² Dept. of Nephrology, Linköping University Hospital, Linköping, Sweden

³ Dept, of Radiology, Linköping University, Linköping, Sweden

Corresponding author:

Martin Larsson

CMIV

University Hospital

581 85 Linköping

Sweden

E-mail: martin@ahlab.se

Telephone: (+46) 733 797 144

Grant support: This study was in part funded by a grant from the Research Council of South-Eastern Sweden (FORSS).

Running title: Renal Artery Stenosis Flow Parameters

ABSTRACT

Purpose. To investigate the feasibility of quantitative parameter extraction from a mathematical model fitted to renal artery magnetic resonance flow data.

Material and methods. Sixteen subjects, 8 patients and 8 normal controls, were examined with cine phase-contrast velocity measurements, and blood flow data from the aorta and both renal arteries were extracted by means of contour detection. A mathematical model with eight parameters describing the time, duration and amplitude of the systolic acceleration and the diastolic deceleration was fitted to the aorta and renal artery blood flow data from each subject. The curve fitting was evaluated with R^2 values. Statistical analysis was performed with unpaired Wilcoxon tests and stepwise logistic regression.

Results. Three data sets out of 48 yielded R^2 values below 0.80 and were considered unreliable for parameter estimation. Basal flow was significantly, and systolic peak amplitude almost significantly, lower in stenotic arteries. Logistic regression indicated that two parameters describing basal flow and the duration of acceleration can accurately predict stenosis.

Conclusion. The results suggest that it is technically feasible to fit a mathematical model to renal blood flow data, extracting quantitative parameters that may prove useful for quantification and diagnosis of renal artery stenosis.

Key words. Flow measurement; Magnetic Resonance Angiography; Blood flow; Renal artery stenosis.

INTRODUCTION

Renal artery stenosis is a well known cause of high blood pressure. However, recent studies suggest that renal artery stenosis may also be a cause of impaired renal function and renal failure (1). X-ray digital subtraction angiography (DSA) has long been considered the gold standard for the diagnosis of renal artery stenosis. Although providing images with high spatial resolution, the technique is limited to a few two-dimensional projections, making assessment of a suspected stenosis difficult. The X-ray DSA method is also invasive and employs nephrotoxic contrast agents that might cause permanent renal failure in a patient with impaired renal function (2).

In contrast with X-ray DSA, three-dimensional gadolinium-enhanced magnetic resonance angiography (3D-Gd-MRA) provides several advantages, in particular for patients with renal failure or transplanted kidneys (3-7). The procedure is non-invasive and the gadolinium-based contrast agents used in 3D-Gd-MRA are not nephrotoxic when the correct dosage is used (2, 8, 9). The clinical value of 3D-Gd-MRA is now well documented (10-14). Two recent meta-analyses have shown sensitivity and specificity values above 90% and an ROC area of 0.99, respectively, relative to the reference method invasive angiography (15-16). Recent technical developments in 3D-Gd-MRA acquisition technique include the introduction of time-resolved sequences and injection protocols tailored to the specific acquisition scheme (17-19). For presentation of results, new methods for adapting volume rendering protocols to the varying grayscale in MR images have been proposed (20-21).

Although 3D-Gd-MRA produces images with lower spatial resolution than X-ray DSA, MR imaging can be used to acquire projections in any three-dimensional plane. In addition,

functional information about blood flow, flow pattern and renal perfusion may be obtained in one single examination. The diagnostic information is therefore not limited to morphologic changes alone.

In particular in cases where the morphological findings are equivocal, renal artery blood flow data may provide valuable additional diagnostic information. A number of studies have demonstrated reduced mean flow in the renal arteries in patients with renal artery stenosis and this has been proposed as a way of predicting the outcome of angioplasty (22-26). However, since the mean flow through the renal parenchyma remains fairly constant even for severe renal artery stenosis due to the autoregulatory capacity of the kidney (27), the mean flow parameter alone may not be sufficient for classification of a stenosis as hemodynamically significant. Hence, it may be relevant to study not only the mean value of the blood flow, but also its temporal course during the cardiac cycle. However, it is not immediately clear how to quantitatively assess differences in flow waveforms which may be visually quite obvious.

It has been shown that patients with renal artery stenosis have lower diastolic flow, more damped systolic peaks and longer wave duration (28). Schoenberg et al have in several papers investigated the use of blood flow profile curves as a method for diagnosis of renal artery stenosis (29, 30, 31). These curves are divided into four characteristic sections, from which relevant diagnostic information can be inferred ([Figure 1](#)). The findings most typical for flow-limiting renal artery stenosis are reduction in mean flow (when compared to the aorta) and delay or absence of the early systolic peak. The loss or delay of the early systolic peak is considered a more sensitive marker for renal artery stenosis which can be detected before the reduction in mean renal artery flow occurs (30).

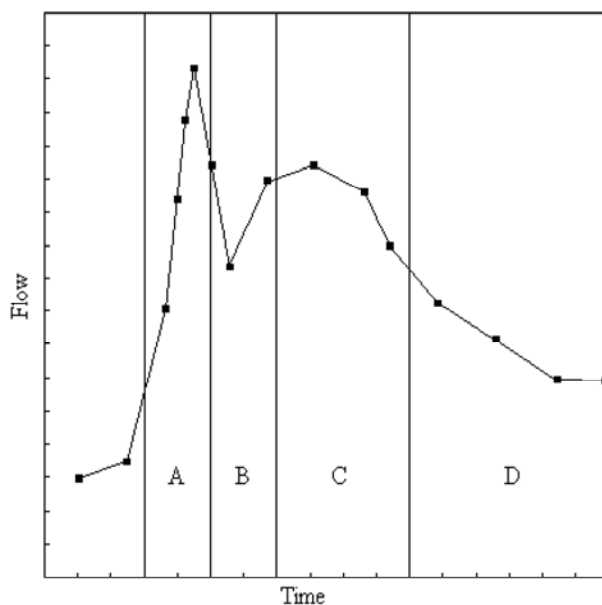


Figure 1. Schematic of a renal blood flow profile curve (drawn by free hand after Schoenberg et al (29), with permission). The blood flow curve shows an early systolic peak (A) followed by an "incisure" (B), a midsystolic peak (C) and a diastolic phase (D).

As long as the analysis of the shape of blood flow profile curves is carried out visually it is, in contrast to quantitative analysis of mean flow or mean velocity, subject to interobserver variability. By fitting a mathematical model to the curve data using non-linear regression, it could be possible to extract quantitative parameters corresponding to the visual findings, hopefully eliminating one source of measurement variability. The ideal model is one that includes the necessary parameters, such as delay, duration and amplitude of the early systolic peak, without being too complex.

The aim of this study was to investigate whether it is feasible to use a mathematical model to extract quantitative parameters from MR blood flow curves. This may in the future prove useful for diagnosis and quantification of renal artery stenosis.

MATERIALS AND METHODS

Subjects

The study material consisted of two groups of subjects. The first group consisted of 8 patients, 2 females and 6 males aged 49-82 years with a mean age of 69.8 years. In this group, all patients had a serum creatinine level of 150–300 $\mu\text{mol/L}$ (1.7–3.4 mg/dL) and had drug-treated hypertension with >160 mmHg systolic blood pressure and/or >90 mmHg diastolic blood pressure. They also had a clinical suspicion of renal artery stenosis according to one or several of five criteria: general vascular disease (previous coronary disease, cerebrovascular disease, symptomatic lower extremity atherosclerosis), sudden onset or exacerbation of hypertonic disease, unmanageable hypertonic disease despite treatment with three drugs, hypertonic disease with retinopathy grade III or IV or rise in serum creatinine in response to treatment with angiotensin-converting enzyme (ACE) inhibitors or angiotensin II receptor (ATII-R) inhibitors. Renal artery stenosis was confirmed in all eight patients by means of CT angiography as more than 50% diameter reduction of one or both of the renal artery lumina (32).

The control group consisted of 8 subjects, 6 females and 2 males, aged 39-62 years with a mean age of 51.6 years with no suspicion of renal artery disease who went through 3D-Gd-MRA as part of investigations prior to kidney donation. In all these cases, the morphological findings at 3D-Gd-MRA were normal.

Informed written consent was obtained from every subject.

Image acquisition and flow data extraction

The examination procedure was carried out on a 1.5 T scanner (Philips Intera Achieva Nova Dual) with an effective gradient strength of 114 mT/m using a SENSE Body coil. After axial Balanced Turbo Field Echo (b-TFE) images and coronal 3D-Gd-MRA (TE=1.54 ms, TR=5.4 ms, 3 dynamic scans) of the renal arteries, quantitative flow measurements were made in the abdominal aorta, immediately cranial to the renal arteries, and in both renal arteries, with a Fast Field Echo sequence, using ECG triggering, 32 cardiac phases, voxel size $1.2 \times 1.2 \times 6$ mm³, TE =5.3 ms , TR=8.6 ms and a velocity encoding value (v_{enc}) of 200 cm/s. The gating method used was retrospective cardiac synchronization by vector cardiography.

The quantitative flow measurements were planned on the Maximum Intensity Projection (MIP) images of the first dynamic 3D-Gd-MRA scan of the aorta and the renal arteries as well as on the b-TFE images. The acquisition slice was placed perpendicular to each vessel. If a stenosis was seen on the MIP images, the slice was, whenever possible, placed proximal to the stenosis, where disturbed flow is expected to be less pronounced. However, in cases with very proximal stenoses, the slice was instead placed several cm distal to the stenosis to avoid the frequently turbulent region immediately downstream (33). The subject was allowed to breathe freely during the acquisition, which took approximately 2 min (depending on the heart rate).

The 2D phase-contrast cine images were transferred to a workstation (Philips ViewForum) and analyzed by means of contour detection. In brief, an ellipse was drawn on free-hand around the vessel of interest, and the program then determined the boundaries of the vessel and extracted flow values (in ml/s) from each of the 32 phases, thus automatically adjusting for variations in vessel position during the cardiac cycle.

Model fitting and analysis

The data was then entered into a curve fitting program (WinCurveFit 1.1.8, Kevin Raner Software) on a PC/Windows workstation. The program uses the quasi-Newton Davidon-Fletcher-Powell algorithm when performing non-linear regression.

The mathematical model used in the curve fitting is described in Eqn. 1, [Figure 2](#) and [Table 1](#).

$$Q(t) = a + b \times \tanh\left(\frac{t-c}{d}\right) - b \times \tanh\left(\frac{t-e}{f}\right) - \frac{g}{\frac{(t-h)^2}{200} + 1} \quad \text{Eqn. 1}$$

The model consists of three components in addition to the baseline value. The first hyperbolic tangent function corresponds to the ascent of the systolic peak, the second, negative hyperbolic tangent function corresponds to the descent of the systolic peak and the third, negative term corresponds to the post-systolic incisure. Note that the position in time of this incisure can be adapted freely to the measured data and thus accommodated to both early and late depressions in the curve after the systolic peak. The number 200 in Eqn. 1 represents the duration of the post-systolic incisure. The duration was fixed to a constant in order to keep the number of parameters to a minimum. The value 200 ms is an approximation based on all the blood flow data sets.

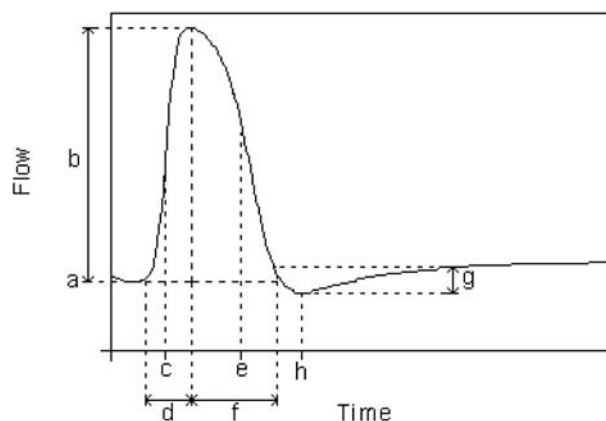


Figure 2. A schematic of the mathematical model and its parameters. The parameters *a* through *h* correspond to those in Table 1. The curve is plotted using the mathematical model and therefore differs somewhat from the curve in [Figure 1](#).

The model was fitted to the aortic and renal artery blood flow data from each subject. Initial values were entered for each data set by the first author (in some cases several initial values were tried until an acceptable fit was obtained). The aim was to produce a curve as close to the data points as possible. The fitted curves were then evaluated for goodness of fit based on the R^2 value, and R^2 values of at least 0.80 were considered acceptable.

For each study group, mean values of the parameter estimates were calculated. In the patient group, the renal artery with significant stenosis was used for calculation of mean values. In this group, one patient was excluded on account of the R^2 value being less than 0.80. In the control group, the right renal artery was used for calculations.

Statistical analysis was performed with unpaired Wilcoxon tests and with a stepwise logistic regression model predicting Normal or Stenotic finding from the 8 estimated parameters. This calculation was performed with JMP 6.0 (SAS Institute Inc, Cary, NC, USA).

Table 1. *The model parameters and their corresponding curve components.*

Parameter	Model component
<i>a</i>	The baseline of the model
<i>b</i>	The amplitude of the ascent and descent of the systolic peak
<i>c</i>	The time-point for the ascent
<i>d</i>	The duration of the ascent
<i>e</i>	The time-point for the descent
<i>f</i>	The duration of the descent
<i>g</i>	The amplitude of the post-systolic incisure
<i>h</i>	The time-point for the post-systolic incisure

RESULTS

In the eight patients, who all had a stenosis reducing the diameter of either renal artery by at least 50%, four patients had a normal contralateral renal artery, whereas four had an artery with a diameter reduction less than 50%. In no case were there bilateral morphologically significant stenoses. Five of the patients had accessory renal arteries; in those cases the largest vessel on either side was used for flow measurements.

In total, sixteen subjects with 3 data sets each were analyzed in this study. The mean values of the cross-sectional area and number of pixels in the areas used for flow measurements are shown in [Table 2](#). Three data sets from three different patients yielded an R^2 value less than 0.8 and were considered unreliable for parameter extraction and hence excluded from the subsequent analysis.

Table 2. Characteristics of the area used for blood flow measurements. Values are given as means (standard deviation) for all 16 subjects.

Vessel	Cross-sectional area (mm ²)	Number of pixels
Aorta	393 (108)	287 (78)
Right renal artery	74 (27)	54 (19)
Left renal artery	79 (31)	58 (23)

A summary of the measured blood flow data is presented in [Table 3](#).

MIP 3D-Gd-MRA images and flow curves of three of the subjects, considered as normal, pathological, and inconclusive, respectively, are shown in [Figure 3](#), [Figure 4](#) and [Figure 5](#).

Curves based on the mean values of the estimated parameters for the two groups are shown in [Figure 6](#).

Comparing parameter values between the two groups, significant differences were present for a (baseline flow; $p < 0.01$), which was lower, and h (time for post-systolic incisure; $p < 0.05$), which was higher for the stenotic renal arteries than for those of normal controls. The amplitude of the systolic peak (b) had a tendency toward lower values for stenotic arteries ($p = 0.053$). The stepwise logistic regression resulted in a model with two significant independent variables: a and d (duration of acceleration) (both $p < 0.01$). As seen in [Figure 7](#), the combination of these two parameters was able to accurately predict normal or stenotic finding in all 14 cases.

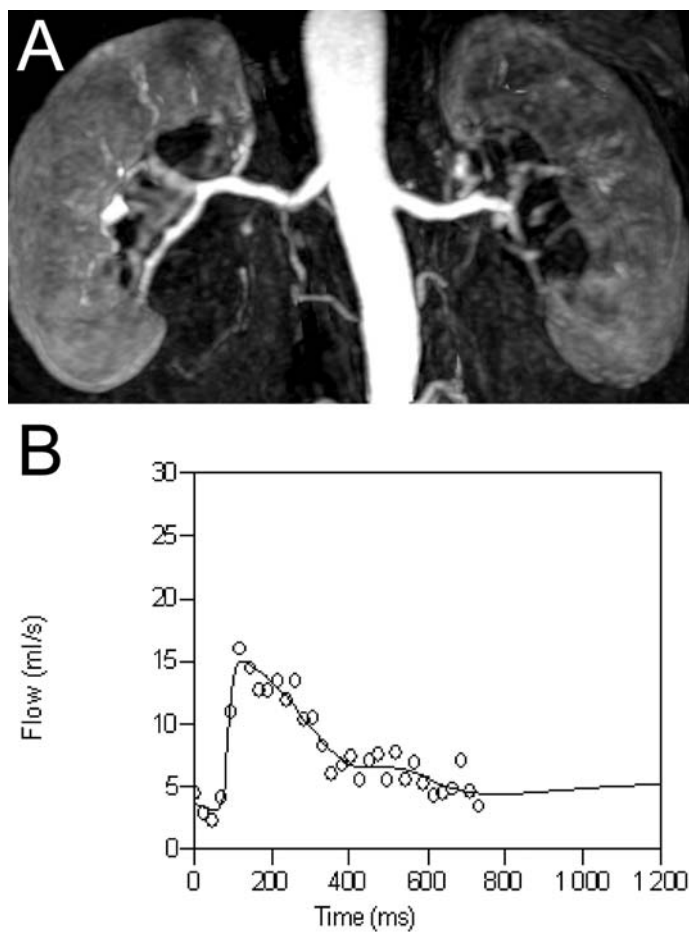


Figure 3. Coronal 3D-Gd-MRA MIP image of subject with morphologically normal renal arteries (A). Flow curve from the right renal artery (B).

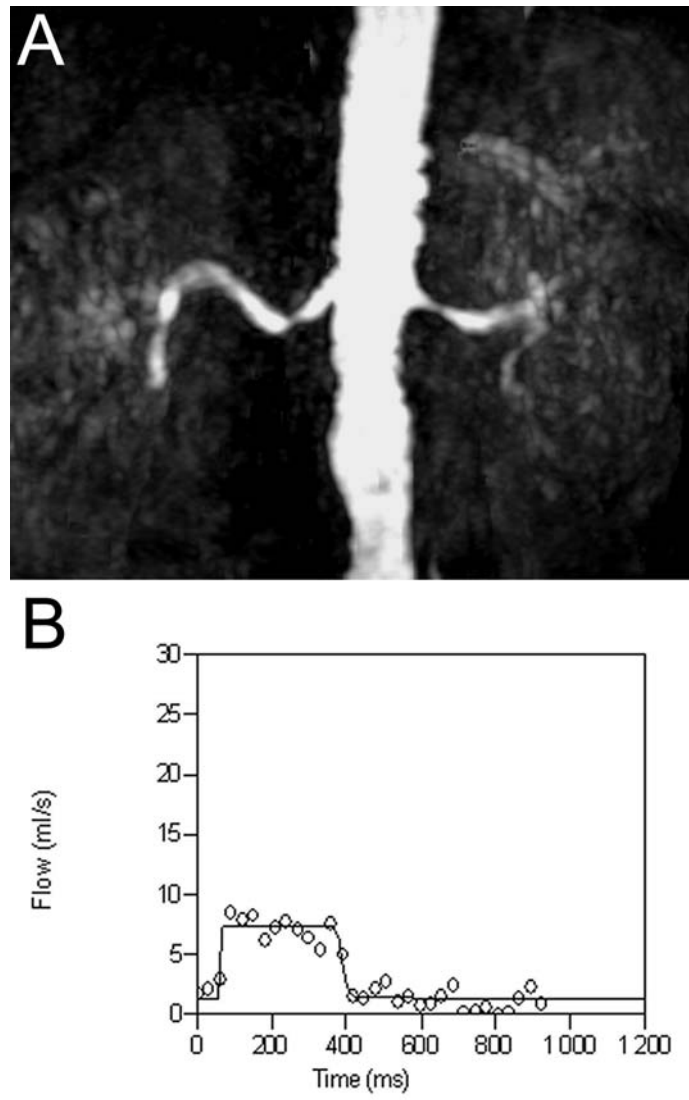


Figure 4. Patient with right-sided significant stenosis and left-sided non-significant stenosis, coronal 3D-Gd-MRA MIP image (A). Flow curve from the right renal artery (B).

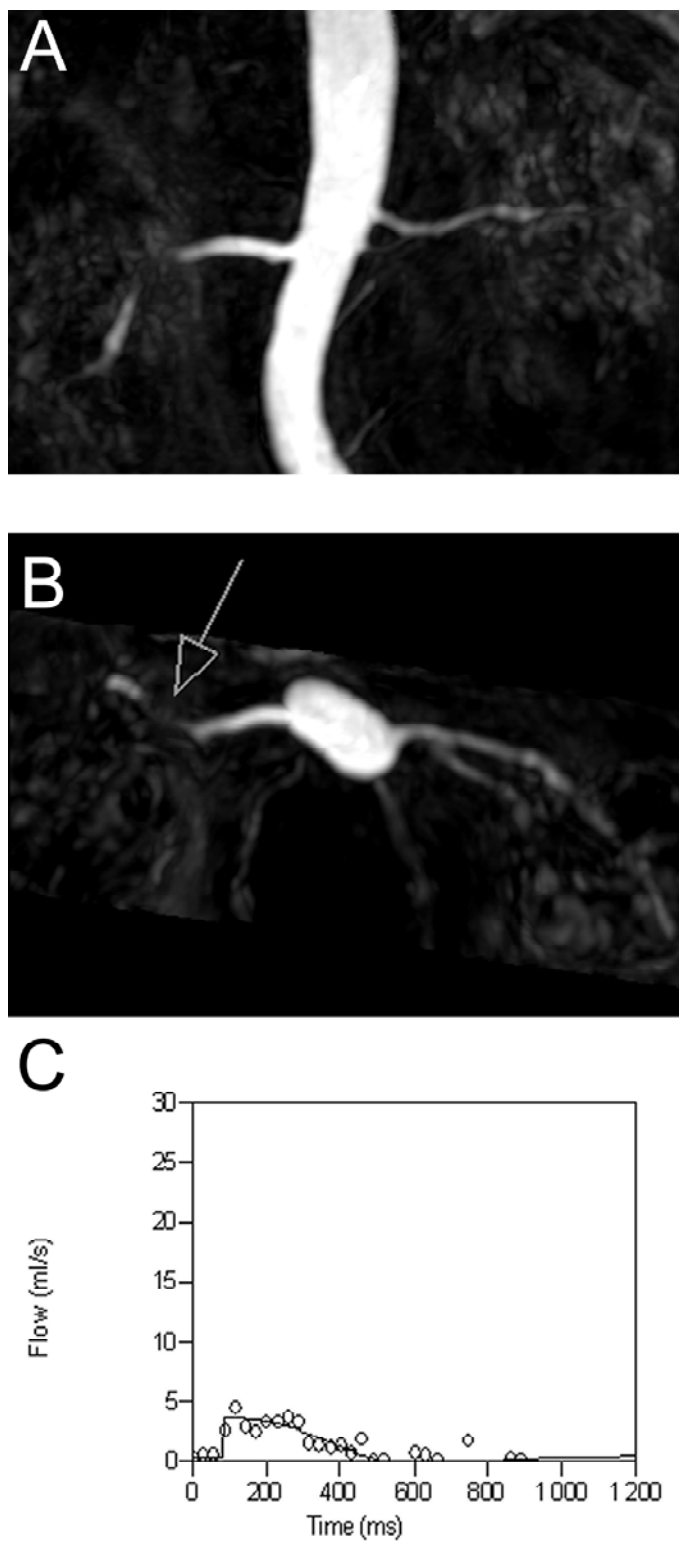


Figure 5. Patient with renal artery stenosis in the right artery, not well seen in coronal MIP image (A) but clearly visible in axial MIP image (B). Note accessory artery on left side. The patient was diagnosed with polycystic renal disease. Flow curve from the right renal artery resulting in an R^2 value of 0.75 (C).

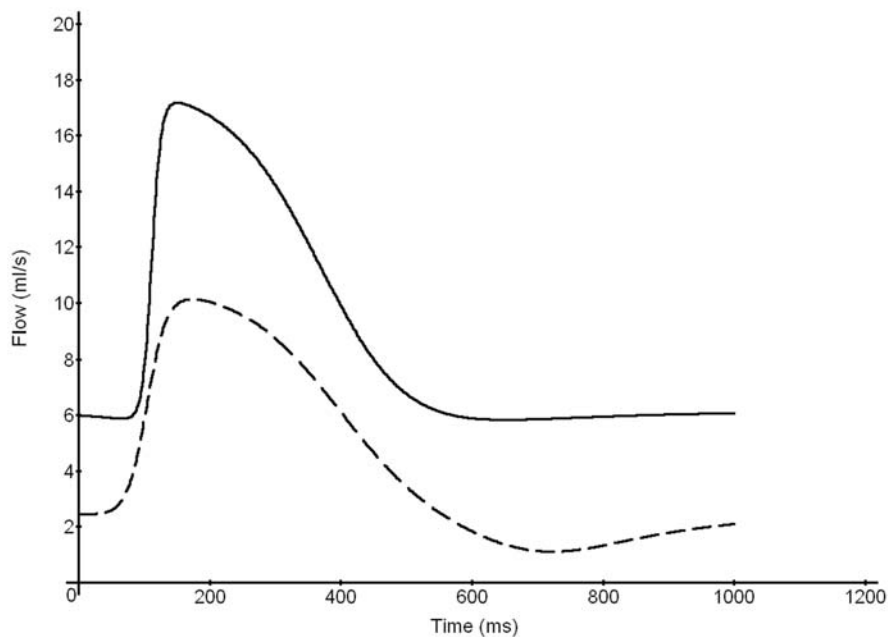


Figure 6. Plotting of Eqn. 1 using calculated mean parameter estimates shown in [Table 3](#). Solid line shows estimates with stenosis (most diseased side), dashed line shows estimates without stenosis (right renal artery).

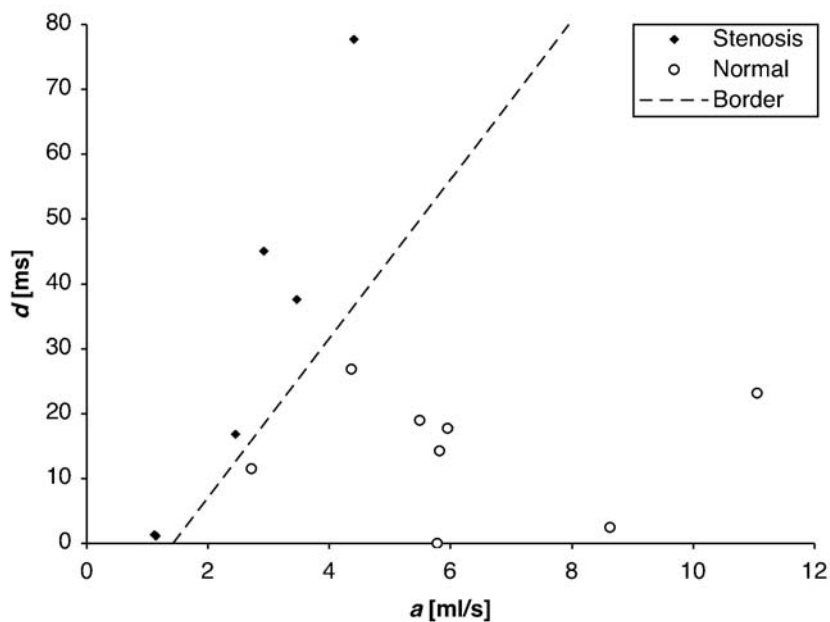


Figure 7. Plot of estimated a and d values for stenotic arteries (most diseased side) and normal controls (right side). The dashed line denotes the border between the regions where the logistic regression model predicts stenosis and normal finding, respectively.

Table 3. The means of the estimated parameters a – h for each group, the mean of their standard errors and their standard deviations; and the mean explanatory value (R^2) of the model. Three datasets yielded R^2 -values below 0.80 and were excluded from the analysis.

			a	b	c	d	e	f	g	h	R^2
Patients	n										
Aorta	8	Mean of estimates	13.0	72.3	107.8	31.5	387.6	89.1	45.4	346.3	0.98
		Mean of standard errors	5.4	25.2	29.2	4.5	144.6	44.3	28.2	75.7	
		Standard deviation of estimates	2.9	6.6	3.1	6.1	12.4	14.5	10.5	42.3	
Most diseased side	6	Mean of estimates	2.6	4.1	104.7	30.0	396.2	147.5	1.6	704.9	0.88
		Mean of standard errors	1.3	1.2	49.1	29.6	149.5	137.1	3.2	189.1	
		Standard deviation of estimates	0.6	1.0	11.6	24.2	42.7	43.5	0.8	239.0	
Least diseased side	7	Mean of estimates	2.0	4.4	86.6	5.3	329.6	74.7	-1.8	478.0	0.93
		Mean of standard errors	1.9	2.1	34.0	10.4	51.1	75.1	2.2	101.7	
		Standard deviation of estimates	0.4	0.6	19.0	164.1	19.2	23.5	0.8	121.5	
Normals	n										
Aorta	8	Mean of estimates	35.0	95.9	116.7	29.4	376.4	111.1	106.1	343.8	0.98
		Mean of standard errors	28.5	37.0	10.6	10.6	131.9	44.8	143.5	57.1	
		Standard deviation of estimates	4.4	12.4	2.9	6.6	30.0	19.0	21.0	67.3	
Right renal artery	8	Mean of estimates	6.2	5.9	112.1	14.4	368.4	139.0	1.0	475.1	0.94
		Mean of standard errors	2.6	1.7	13.2	9.4	199.1	80.4	5.2	153.6	
		Standard deviation of estimates	0.5	1.3	6.4	21.4	42.0	67.5	1.6	150.3	
Left renal artery	8	Mean of estimates	5.2	10.7	111.8	13.3	392.5	131.7	0.0	506.4	0.94
		Mean of standard errors	1.7	14.6	16.4	15.1	186.0	65.4	4.6	128.8	
		Standard deviation of estimates	0.6	151.8	12.0	35.8	46.5	63.6	1.4	85.4	

DISCUSSION

When assessing renal artery blood flow profile curves, two different approaches may be used. The blood flow can be evaluated by a visual method, or by quantitative measurement of the relevant parameters. The method evaluated in this study is an example of a quantitative approach based on the visual appearance of the flow curve.

The results from this study suggest that it is feasible to use a mathematical model to extract quantitative parameters from time-resolved renal blood flow data. This more objective method to describe the shape of the flow curve could in the future prove useful for diagnosing renal artery stenosis. If this leads to a reduction in the number of X-ray DSA procedures, patients – in particular those with renal failure – would benefit from less exposure to invasive procedures, radiation and nephrotoxic contrast agents.

However, it is important to make clear that no physiological assumptions have been made concerning the renal blood flow profile and the model and its parameters. Therefore, it remains to investigate what diagnostic conclusions can be drawn from these parameters.

Image acquisition and curve calculation

The flow measurements in this study were made with ECG triggering and with the patient breathing freely. While this ought to produce some blurring of the images, it was assumed that an acceptable mean value of the flow over the cross-sectional area was obtained. The alternative of performing the measurements during one breath-hold would not have permitted the temporal resolution within the cardiac cycle that we considered necessary. Avoiding blurred images is probably more important when assessing the morphology of a suspected stenosis.

A problem with our velocity measurements was the rather high noise level in the flow curves, as illustrated by [Figures 3-5](#). Our visual impression is that a large part of the explanation lies in difficulties in delineating the cross-section of the arteries rather than in inherent signal-to-noise limitation in the images. Judging from the curves in other publications (28, 29), this seems to be a common problem of the phase-contrast method. This was one of our major rationales for creating an analysis method less sensitive to noise in the curves. An alternative solution might be better algorithms for vessel segmentation.

The presence of gadolinium contrast media in the blood is not a requirement when measuring blood flow with MR. In this study, it is merely a consequence of the gadolinium-enhanced MR angiography that was performed before the flow measurements. We assumed that the presence of gadolinium in the subject's blood would not produce any substantial disturbance in the flow measurements, since the phase angle (which forms the base for the velocity measurement) is not expected to be affected. Possibly, it might even improve the signal-to-noise characteristics of the velocity data, as the amplitude of the MR signal is expected to increase.

The choice of a velocity encoding value (v_{enc}) of 200 cm/s was made in order to reduce aliasing. However, with adequate algorithms to compensate for aliasing in the post-processing, lower v_{enc} values might, in principle, yield more accurate results.

The mathematical model

The choice of the hyperbolic tangent (tanh) function as a base for the model was based on the visual appearance of a curve drawn through the blood flow data points and not based on any physiological theory. The sigmoid appearance of the tanh function met our needs.

Furthermore, the parameters of the tanh function, such as amplitude and time-point for the

ascent/descent could easily be coupled to corresponding characteristics of the renal blood flow profile. An alternative could be the error function (distribution function of the normal distribution), which shows a similar sigmoid form and can be fitted with the same parameters.

The mathematical model used in our study was designed with the intention to use a minimum of parameters but still make the model complex enough to describe the essential characteristics of the blood flow profile curve. These characteristics include base flow (diastolic flow) and the amplitude of the systolic peak as well as any delay or extended duration of either the ascending or descending part of the curve. As a postsystolic incisure has been described as a central finding (30), this was also included in the model. Further studies are needed to evaluate the optimal design of the model. Future modifications of the model could include both a reduction and an increase in the number of parameters.

The error levels of the model and extracted parameters have not been tested in this study. Tests of the fit performance and associated error levels could be made, e.g., by adding different levels of noise to simulated flow profile curves. However, this is beyond the scope of this study.

Model fitting

Three of our data sets yielded an R^2 value less than 0.80 and were considered unreliable for parameter extraction. This could be due to measurement errors when performing the examination, image quality issues or to errors when extracting flow data with the contour detection method. The data sets seemed to be too scattered to yield a curve that could be used for extraction of relevant parameters.

The choice of initial values could have an impact on the outcome of the results of the curve

fitting. When entering initial values into the curve-fitting program, an initial curve is plotted, thus showing the user whether the initial values produces a curve running close to the data points or not. In most cases, the high R^2 values indicate that the method has converged to the best possible approximation, but in cases with unacceptable fit, it is conceivable that better R^2 values could have been obtained with other initial values. This means that our method does not eliminate all subjective elements. Probably, a higher level of automation, reducing this, may be achieved in future software. The inclusion limit of 0.80 is, of course, also somewhat arbitrary.

The computer program we have used automatically presents the curve fitting parameter estimates together with their standard errors. Although a large value of the standard error suggests a high degree of uncertainty in the estimate, it has not been investigated in this study what impact the standard error may have on the reliability of the parameter estimates. However, this information could prove useful in future studies of the method.

Parameter analysis

The eight different parameters of the model (a through h) can be regarded as approximations of the different parts of the flow profile curve. These approximations are described in [Table 1](#) and in [Figure 2](#).

The extraction of quantitative parameters from renal blood flow data has been suggested in a previous study by Schoenberg et al (29). The parameter in that particular study was $Rmax_{1/2}$, which is defined as the ratio of the first and second systolic maxima. However, the use of a mathematical model fitted to the entire renal blood flow curve is a different approach. It favors extraction of several parameters at once and can hopefully eliminate one source of measurement variability when assessing the hemodynamic significance of the stenosis. The

sensitivity to noise in the curve is expected to be less when the extracted parameters are not determined by one or two values but by the entire curve.

Our blood flow profile curves differ slightly in the general shape compared to those of Schoenberg et al. This could be due to such factors as differences in image acquisition procedures or be due to the selection of our few cases. Whether these differences have any impact on the choice of model or the extraction of parameters needs to be further investigated.

In the mathematical model employed here, the baseline level, amplitude and time-point parameters (a , b , g , c , e and h) can be quite easily interpreted. The meaning of the duration parameters (d and f) is less intuitive. One way to express it is to say that a d -value of 100 ms corresponds to 90% of the ascent taking place in a time interval of 294 ms (and proportionally to this for other durations).

The curves based on mean parameter estimates in each group ([Figure 6](#)) were included as an attempt to visualize any general differences in renal blood flow waveforms. The most obvious differences are a lower base flow level and a less steep acceleration phase in the stenotic vessels. This is another way of expressing the differences between the groups in a and b values (or the inclusion of a and d in the final logistic regression model) and is in line with observations in earlier studies (28, 30). A decreased flow in diastole with progressing disease has also been found with ultrasound in conditions such as renovascular and essential hypertension (34-36). The absence of a visible incisure in the mean curve, at least for healthy subjects, is probably due to superposition of several “dips” with varying delay (as illustrated by the large standard deviation of h)

In this study, no correlation between the flow curves and the clinical degree of renal artery stenosis was made. Such a correlation would be useful in further evaluation of the clinical

relevance of quantitative parameter extraction.

In conclusion, the results from this study suggest that it is technically feasible to use a mathematical model to extract quantitative parameters describing the appearance of MR flow curves. However, further studies are needed to evaluate whether these parameters can be clinically useful as a component in diagnosing renal artery stenosis.

REFERENCES

1. Uzu T, Takeji M, Yamada N, et al. Prevalence and outcome of renal artery stenosis in atherosclerotic patients with renal dysfunction. *Hypertens Res* 2002;25(4):537-42.
2. Morcos SK, Thomsen HS, Webb JAW, et al. Contrast-Media-Induced Nephrotoxicity: a Consensus Report. *Eur Radiol*. 1999;9:1602-1613.
3. Prince MR, Schoenberg SO, Ward JS, Londy FJ, Wakefield TW, Stanley JC. Hemodynamically significant atherosclerotic renal artery stenosis: MR angiographic features. *Radiology* 1997;205(1):128-36.
4. Rieumont MJ, Kaufman JA, Geller SC, Yucel EK, Cambria RP, Fang LS, et al. Evaluation of renal artery stenosis with dynamic gadolinium-enhanced MR angiography. *AJR Am J Roentgenol* 1997;169(1):39-44.
5. Ghantous VE, Eisen TD, Sherman AH, Finkelstein FO. Evaluating patients with renal failure for renal artery stenosis with gadolinium-enhanced magnetic resonance angiography. *Am J Kidney Dis* 1999;33(1):36-42.
6. Smedby Ö, Åsberg B, Eriksson P. Renal artery stenosis in patients with impaired renal function detected with MR angiography. *Eur Radiol* 2003;13, Suppl 1:215.
7. Luk SH, Chan JH, Kwan TH, Tsui WC, Cheung YK, Yuen MK. Breath-hold 3D gadolinium-enhanced subtraction MRA in the detection of transplant renal artery stenosis. *Clin Radiol* 1999;54(10):651-4.
8. Price MR, Arnoldus C, Frish JK. Nephrotoxicity of High-Dose Gadolinium Compared to Iodinated Contrast. *J Magn Reson Imaging*. 1996;6:162-166.
9. Krestin GP, Schuhmann-Giampieri G, Haustein J, et al. Functional Dynamic MRI, Pharmacokinetics and Safety of Gd-DTPA in Patients with Impaired Renal Function. *Eur Radiol*. 1992;2:16-23.
10. Holland GA, Dougherty L, Carpenter JP, Golden MA, Gilfeather M, Slossman F, et al. Breath-hold ultrafast three-dimensional gadolinium-enhanced MR angiography of the

- aorta and the renal and other visceral abdominal arteries. *AJR Am J Roentgenol* 1996;166(4):971-81.
11. Postma CT, Joosten FB, Rosenbusch G, Thien T. Magnetic resonance angiography has a high reliability in the detection of renal artery stenosis. *Am J Hypertens* 1997;10(9 Pt 1):957-63.
 12. Bakker J, Beek FJ, Beutler JJ, Hene RJ, de Kort GA, de Lange EE, et al. Renal artery stenosis and accessory renal arteries: accuracy of detection and visualization with gadolinium-enhanced breath-hold MR angiography. *Radiology* 1998;207(2):497-504.
 13. Willmann JK, Wildermuth S, Pfammatter T, Roos JE, Seifert B, Hilfiker PR, et al. Aortoiliac and renal arteries: prospective intraindividual comparison of contrast-enhanced three-dimensional MR angiography and multi-detector row CT angiography. *Radiology* 2003;226(3):798-811.
 14. Eklöf H, Ahlström H, Boström A, Bergqvist D, Andren B, Karacagil S, et al. Renal artery stenosis evaluated with 3D-Gd-magnetic resonance angiography using transstenotic pressure gradient as the standard of reference. A multireader study. *Acta Radiol* 2005;46(8):802-9.
 15. Tan KT, van Beek EJ, Brown PW, van Delden OM, Tijssen J, Ramsay LE. Magnetic resonance angiography for the diagnosis of renal artery stenosis: a meta-analysis. *Clin Radiol* 2002;57(7):617-24.
 16. Vasbinder GB, Nelemans PJ, Kessels AG, Kroon AA, de Leeuw PW, van Engelshoven JM. Diagnostic tests for renal artery stenosis in patients suspected of having renovascular hypertension: a meta-analysis. *Ann Intern Med* 2001;135(6):401-11.
 17. Schoenberg SO, Bock M, Knopp MV, Essig M, Laub G, Hawighorst H, et al. Renal arteries: optimization of three-dimensional gadolinium-enhanced MR angiography with bolus-timing-independent fast multiphase acquisition in a single breath hold. *Radiology* 1999;211(3):667-79.

18. Amann M, Bock M, Floemer F, Schoenberg SO, Schad LR. Three-dimensional spiral MR imaging: Application to renal multiphase contrast-enhanced angiography. *Magn Reson Med* 2002;48(2):290-6.
19. Maki JH, Prince MR, Chenevert TC. Optimizing three-dimensional gadolinium-enhanced magnetic resonance angiography. Original investigation. *Invest Radiol* 1998;33(9):528-37.
20. Smedby Ö, Öberg R, Åsberg B, Stenström H, Eriksson P. Standardized volume-rendering of contrast-enhanced renal magnetic resonance angiography. *Acta Radiol* 2005;46(5):497-504.
21. Persson A, Brismar TB, Lundström C, Dahlström N, Othberg F, Smedby Ö. Standardized volume rendering for magnetic resonance angiography measurements in the abdominal aorta. *Acta Radiol* 2006;47(2):172-8.
22. Wrazidlo W, Schneider S, Lederer W, Brambs HJ, Werner T, Gottschlich KW, et al. Möglichkeiten und Grenzen der Blutflussquantifizierung peripherer arterieller Gefäße mit der MRT unter Anwendung des Phase-Mapping-Verfahrens. *Röfo* 1992;157(2):175-9.
23. Cortsen M, Petersen LJ, Ståhlberg F, Thomsen C, Søndergaard L, Petersen JR, et al. MR velocity mapping measurement of renal artery blood flow in patients with impaired kidney function. *Acta Radiol* 1996;37(1):79-84
24. Kallinowski F, Schönberg S, Bock M, Knopp MV, Clorius J, Allenberg JR. Erfassung der hämodynamischen Auswirkungen einer Nierenarterienstenose mittels einer MR-Flussmessung. *Langenbecks Arch Chir Suppl Kongressbd* 1997;114:443-4.
25. de Haan MW, van Engelshoven JMA, Houben AJHM, et al. Phase-Contrast Magnetic Resonance Flow Quantification in Renal Arteries – Comparison with ¹³³Xenon Washout Measurements. *Hypertension*. 2003;41:114-118.
26. Binkert CA, Debatin JF, Schneider E, Hodler J, Ruehm SG, Schmidt M, et al. Can MR measurement of renal artery flow and renal volume predict the outcome of

- percutaneous transluminal renal angioplasty? *Cardiovasc Intervent Radiol* 2001;24(4):233-9.
27. May AG, de Weese JA, Rob CG. Hemodynamic effects of arterial stenosis. *Surgery* 1963;53:513-524.
28. Westenberg JJ, Wasser MN, van der Geest RJ, Pattynama PM, de Roos A, Vanderschoot J, et al. Variations in blood flow waveforms in stenotic renal arteries by 2D phase-contrast cine MRI. *J Magn Reson Imaging* 1998;8(3):590-7.
29. Schoenberg SO, Knopp MV, Bock M, et al. Renal Artery Stenosis: Grading of Hemodynamic Changes with Cine Phase-Contrast MR Blood Flow Measurements. *Radiology*. 1997;203:45-53.
30. Schoenberg SO, Knopp MV, Londy F, et al. Morphologic and Functional Magnetic Resonance Imaging of Renal Artery Stenosis: A Multicenter Tricenter Study. *J Am Soc Nephrol*. 2002;13:158-169.
31. Schoenberg SO, Bock M, Kallinowski F, Just A. Correlation of Hemodynamic Impact and Morphologic Degree of Renal Artery Stenosis in a Canine Model. *J Am Soc Nephrol*. 2000;11:2190-2198.
32. Halpern EJ, Rutter CM, Gardiner GA, Jr., Nazarian LN, Wechsler RJ, Levin DB, et al. Comparison of Doppler US and CT angiography for evaluation of renal artery stenosis. *Acad Radiol* 1998;5(8):524-32.
33. Yellin EL. Laminar-turbulent transition process in pulsatile flow. *Circ Res* 1966;19:791—804.
34. Norris CS, Barnes RW. Renal artery flow velocity analysis: a sensitive measure of experimental and clinical renovascular resistance. *J Surg Res* 1984;36(3):230-6.
35. Okura T, Watanabe S, Miyoshi K, Fukuoka T, Higaki J. Intrarenal and carotid hemodynamics in patients with essential hypertension. *Am J Hypertens* 2004;17(3):240-4.

36. Pearce JD, Edwards MS, Craven TE, English WP, Mondt MM, Reavis SW, et al.
Renal duplex parameters, blood pressure, and renal function in elderly people. *Am J Kidney Dis* 2005;45(5):842-50.